KINETIC SELECTIVITY AND COMPETITIVE ADSORPTION ON CARBON NANOTUBE BUNDLES

Jared T. Burde and M. Mercedes Calbi
Department of Physics, Southern Illinois University, Carbondale, IL 62901-4401

Introduction

Though a relatively recent discovery, carbon nanotubes have quickly become a mainstay of carbon nanoscience. For gas adsorption applications, the uniqueness of carbon nanotubes stems from their structure: whereas many carbon structures are irregularly shaped and exhibit a heterogenous pore distribution, nanotubes exhibit a simple, homogenous geometric structure. Due to the precision with which nanotubes can be grown to meet desired specifications, including length, diameter, and lattice constant, along with their tendency to spontaneously form bundles characterized by a triangular lattice (Thess, 1996), it is possible to selectively produce a nanostructure featuring not only a very narrow distribution of pore sizes, but also several unique types of adsorption sites.

The degree of regularity seen in each nanotube and the uniformity among nanotubes in a bundle makes possible the existence of a range of interesting phenomena (Calbi, 2001). The grooves that form between adjacent tubes on the outside of the bundle allow the formation of one-dimensional and quasi-one-dimensional phases (Talapatra, 2001; Teizer, 1999; Wilson, 2003), which can then transition into two-dimensional films at higher coverages (Calbi, 2001), when the particles spread to cover the rest of the external surface of the tubes. Other novel phases may form inside the tubes, in the case of nanotubes that have been opened through chemical or mechanical means, and in the interstitial channels (ICs), which exist between neighbouring tubes on the interior of the bundle. In these sites, one-, two-, and three-dimensional phases can form (Ancilotto, 2005), depending on the ratio between the diameter of the adsorbate and the nanotube. In all of these adsorption sites there exists a unique possibility to observe both the novel phases of matter that may form and the transitions between these phases. It is this potential, along with the wealth of applications that may stem from it, which has fueled the intense scientific study of nanotubes.

Though isotherm experiments have helped elucidate the equilibrium characteristics of carbon nanotubes, comparatively little work has been done regarding the kinetics of adsorption (Calbi, 2005). In a recent work, we used computer simulations employing the Kinetic Monte Carlo algorithm to track the behaviour of a gas as it adsorbed on a bundle of nanotubes (Burde, 2007). Our simulations showed a difference of almost two orders of magnitude between the equilibration times for adsorption on external sites, like the grooves and external surfaces of the nanotubes, and internal sites, like interiors of the tubes and the ICs, which had to be reached through diffusion from the ends. This shows the importance of this kinetic point of view; though two systems, one of external sites and the other of internal, may have very similar equilibrium configurations based on the binding energies and chemical potentials involved, their behaviour as they equilibrate, particularly the waiting times required, can be very different.

Another important discovery in our previous work was the dependence on the equilibration time on the binding energy and temperature of the system. For a single line of independent adsorption sites, we observed a linear relationship between the final coverage of the system and the waiting time needed for the system to reach equilibrium. The slope of this line was dependent on the quantity $\exp(\beta\varepsilon)$, where ε represents the binding energy and β is the inverse of the temperature. Because of this, we can expect to find faster adsorption rates and shorter waiting times for systems with lower binding energies and higher temperatures. This critical first step in understanding the kinetics of adsorption on carbon nanotubes bundles laid the foundation for our continuing research in this area.

In our current work, we investigate competitive adsorption between different chemical species, endeavouring to determine the effect of kinetic selectivity on the time evolution of the composite system. After reaching equilibrium at the same chemical potential, the species with the greater binding energy will enjoy the highest coverage. However, the results of our previous work show us that the species with the lower binding energy will exhibit a faster adsorption rate and can therefore briefly achieve a higher coverage than it will be able to maintain at equilibrium. This 'overshoot' will be reached at a time long before the system equilibrates. Our research focuses on characterizing the overshoot (defined as n_{peak}/n_{eq})

and the overshoot time (defined as the time at which the peak overshoot is reached) as functions of the temperature, chemical potentials, and binding energies of the system. To accomplish this, we consider a binary mixture of gases adsorbing on a one-dimensional array of sites, allowing comparisons with our previous results. The knowledge gained in this work will be an important foundation for any application of nanotubes for kinetic separation of gases.

Application of Kinetic Monte Carlo Algorithm to Lattice-Gas Model

A lattice, consisting of a chain of N_s sites, is used to represent the one-dimensional nature of the adsorption sites considered in this model. Each site is assigned a fixed binding energy for each chemical species. Assuming simple, spherical adsorbate particles, we allow only single-site occupation. Then, the total energies E_{Ai} and E_{Bi} for particles of chemical species A and B on a site i are found as:

$$E_{Ai} = \varepsilon_{Ai} + J_{AA} \sum_{j,NN} s_{Aj} + J_{AB} \sum_{j,NN} s_{Bj} \quad [1]$$

$$E_{Bi} = \varepsilon_{Bi} + J_{AB} \sum_{j,NN} s_{Aj} + J_{BB} \sum_{j,NN} s_{Bj} \quad [2]$$

with ε_{Ai} and ε_{Bi} representing the adsorption energies, J_{AA}, J_{AB}, and J_{BB} representing the interaction energies between particles of each chemical species, and s_{ij} taking on the value 1 if a particle of species i is in the adjacent site j and 0 if that site is unoccupied.

With the lattice set up and the site energies determined, we allow the system to evolve using the Kinetic Monte Carlo (KMC) algorithm, selecting the changes in state by the transition probabilities W_{ij}. The calculations used to determine these probabilities are discussed in detail in our previous work, as are the specifics of our application of the KMC algorithm.

Kinetic Selectivity in External Phases

The lattice-gas model that we employ in this work allows us to take into account many different factors that may affect the adsorption behaviour of a carbon nanotube bundle. In order to provide ourselves with the best basis of comparison on the relative importance these variables, however, we begin with the simplest arrangement possible. In this scheme, we use a single chain of adsorption sites, each with a fixed binding energy for each chemical species. By using a homogenous lattice, as well as neglecting the particle-particle interactions, we can consider each adsorption site to be completely independent of its neighbours, allowing us to derive a purely analytical solution. Though this model is too simple to accurately describe a real system, it plays a pivotal role in providing an important baseline to which we can compare the changes in behaviour resulting from the inclusion of other factors at later stages of the research.

Analytical Calculations

In our previous work, we showed that, for the simplest scheme, the kinetics of adsorption on a single line of independent sites is governed by the rate equation:

$$\frac{dn}{dt} = W_{ads}(1-n) - W_{des}n \quad [3]$$

The rate of change of coverage of the system depends on the combination of the probability of adsorption and the number of sites available, as well as the probability of desorption and the number of occupied sites. In our current work, in which we deal with two different coverages for two distinct chemical species, we have extended this equation to include both species so that:

$$\frac{dn_A}{dt} = W_{ads,A}(1 - n_A - n_B) - W_{des,A}n_A \quad [4]$$

$$\frac{dn_B}{dt} = W_{ads,B}(1 - n_A - n_B) - W_{des,B}n_B \quad [5]$$

By solving both differential equations simultaneously, it was possible to obtain equations for the coverage of each chemical species, given by:

$$n_A(t) = C_{A1}e^{-r_1 t} + C_{A2}e^{-r_2 t} + n_{eq,A} \quad [6]$$

$$n_B(t) = C_{B1}e^{-r_1 t} + C_{B2}e^{-r_2 t} + n_{eq,B} \quad [7]$$

In the above equations, the coefficients and time constants can be calculated from the transition probabilities and thus depend on the thermodynamic properties of the system. The twin exponential terms explain the overshoot of the weaker species predicted earlier. The equilibrium coverages $n_{eq,A}$ and $n_{eq,B}$ are found from as:

$$n_{eq,A}(T,\mu) = \frac{1}{1 + e^{\beta(\varepsilon_A - \mu_A)} + e^{\beta(\varepsilon_A - \varepsilon_B)}} \quad [8]$$

$$n_{eq,B}(T,\mu) = \frac{1}{1 + e^{\beta(\varepsilon_B - \mu_B)} + e^{\beta(\varepsilon_B - \varepsilon_A)}} \quad [9]$$

These analytical calculations provide an important validation of the application of the KMC algorithm. By comparing the kinetic behaviour and equilibrium values seen in our simulations to those predicted by these equations, we are able to verify the accuracy of our algorithm.

Simulation Results

The first simulations run for this model serve to create a basis of comparison for further work. In these runs, we use a homogenous line of independent adsorption sites. Figure 1 shows a typical simulation run. The points represent simulation data and the solid lines show the fitted curves calculated from Eqs. 10 and 11. As can be seen, there is a good agreement between the theoretical and simulated behaviours. The weaker species experiences a major overshoot before falling back to its equilibrium, as predicted in our model. The slight deviations observed at equilibrium are an effect of the finite nature of the lattice; by increasing the length of the lattice, it was possible to make them disappear completely, though at the cost of significant computing power.

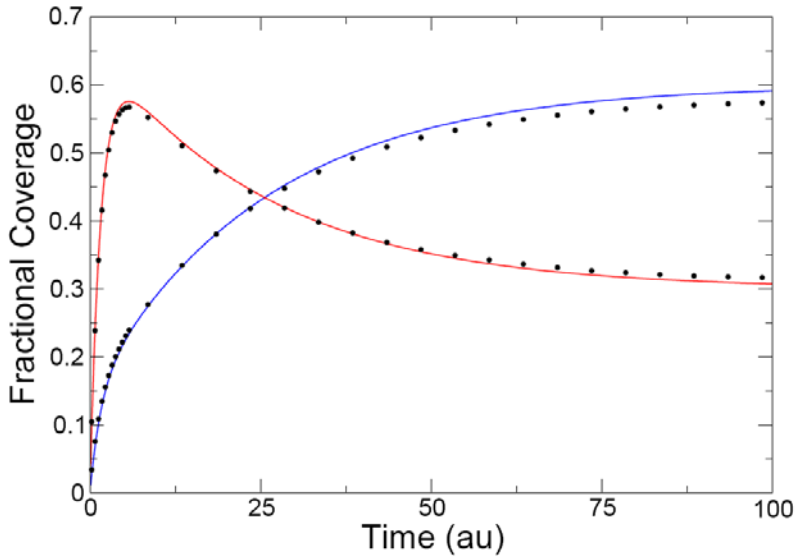

Figure 1: Fractional coverage as a function of time for two chemical species, one (upper curve) with twice the binding energy of the other (lower curve).

With the validation of the model and simulation code, we consider the effect of the system parameters on this overshoot. By fixing the equilibrium coverage of the stronger binding species, we can demonstrate the effect of the weaker species' coverage on the percent overshoot experienced. As shown in Figure 2, the overshoot increases with the equilibrium coverage and the time at which the overshoot is achieved decreases, going to zero as the system approaches a monolayer. The second panel shows the increase in the percent overshoot as the equilibrium coverage of the weaker species is increased.

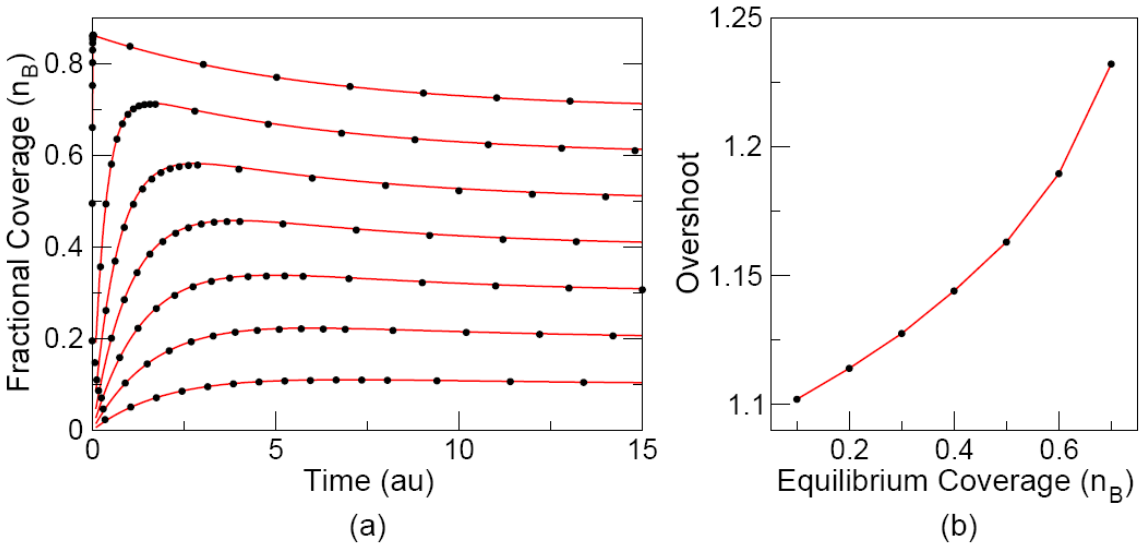

Figure 2: The time evolution of the weaker binding species for a fixed coverage of the stronger species . The overshoot time goes to zero at high coverages (Panel a), while the overshoot increases (Panel b).

Though it increased along with increasing coverage of the weaker binding species, the overshoot also shows a dependence on the coverage of the stronger species. The overshoot also increases with the coverage of the stronger binding species, but to a far greater extent, as shown in Figure 3. Thus, the true maximum of the percent overshoot is achieved for the highest coverages of the stronger species.

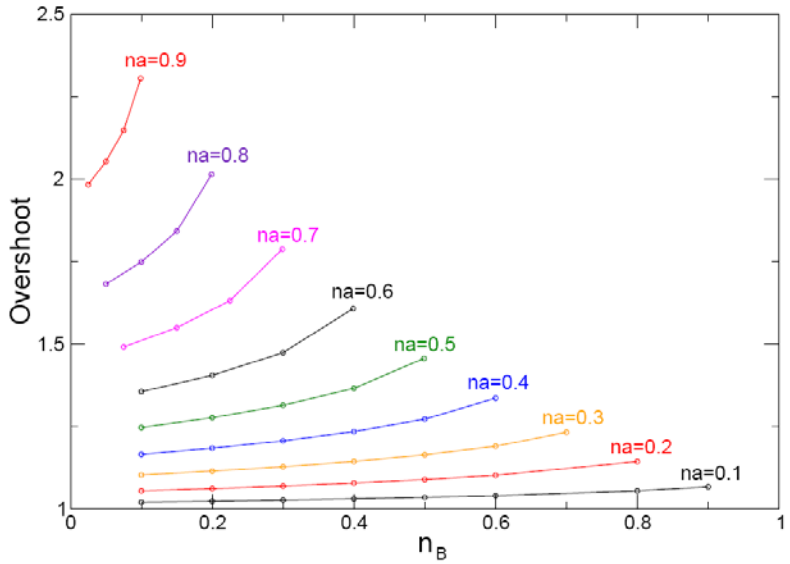

Figure 3: The percent overshoot of the system as a function of the coverage of the weaker binding species for various values of n_A. Though the overshoot increases with increasing n_B, it experiences a far greater effect from increases in the coverage of the competitor.

In addition to looking at the dependence of the coverage (and from it, the chemical potential), we also investigate the role of the binding energy. In these simulations, we fixed the coverages of both species and changed the binding energies. Figure 4 shows the results from these simulations. As the magnitude of binding energy of the weaker species decreases, the system sees an increased overshoot occurring at an earlier time. This overshoot increases even more as the binding energy of the stronger species increases, as the second panel shows.

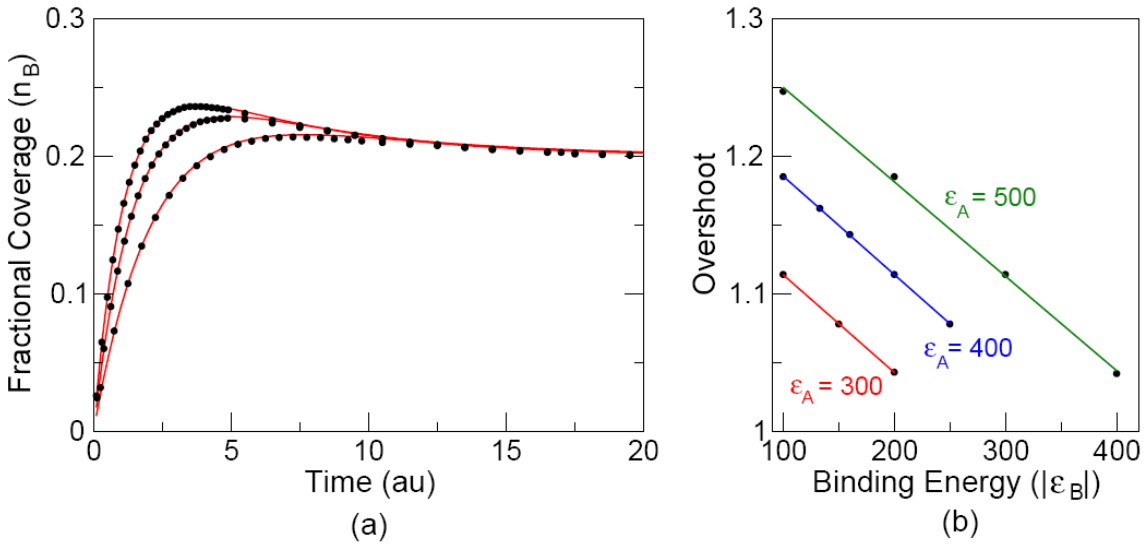

Figure 4: Fractional coverage as a function of time for the weaker binding species with binding energies of -100 K (top), -150 K (middle), and -200 K (bottom). Panel b shows the overshoot as a function of binding energy ε_B for several values of ε_A.

Finally, we looked at the dependence of the overshoot on the temperature of the system. Under these conditions, the equilibrium coverages and binding energies of both species are fixed and the temperature is adjusted. The greatest overshoot is reached at the lowest temperature, which also exhibits

the longest overshoot time. As the temperature increases, the overshoot becomes less pronounced and occurs much earlier in the evolution of the system. Figure 5 shows this effect, while the second panel shows how the magnitude of the overshoot decreases as the temperature goes up.

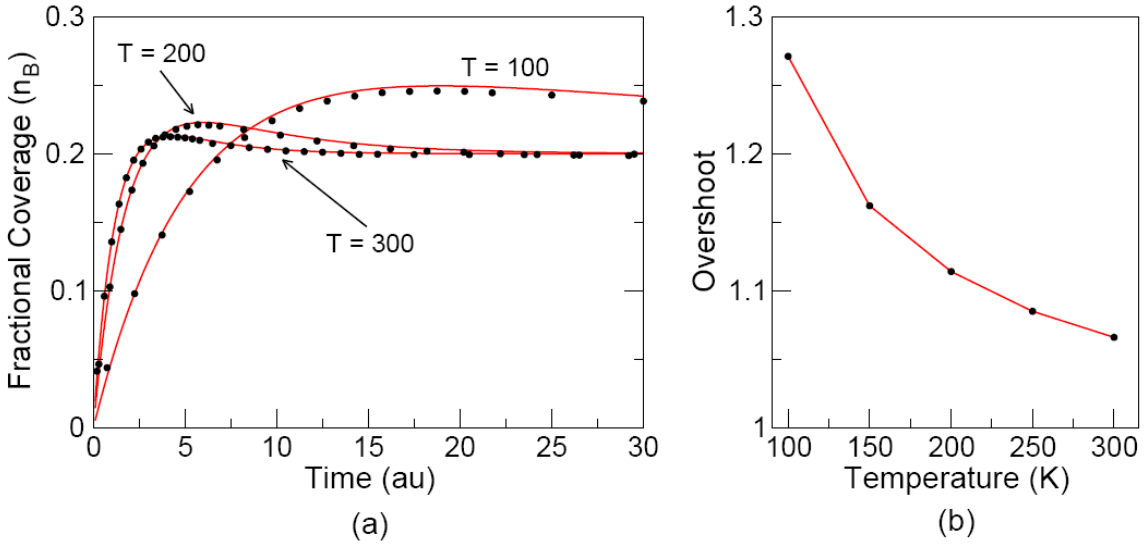

Figure 5: Fractional coverage as a function of time for various system temperatures. In Panel b we see the decrease in the percent overshoot with increases in temperature.

Discussion and Conclusion

The simulations run in this project show that the overshoot and overshoot time depend on the system parameters of chemical potential, binding energy, and temperature. We have shown that the highest overshoots occur when there is a large difference between μ_A and μ_B, which leads to a large ratio between their equilibrium values. More importantly, we see an increase in overshoot as the binding energy of the weaker species decreases and the binding energy of the stronger species increases. This is expected from the dependence on the quantity $\beta\varepsilon$ seen in our previous work. As the binding energy of the weaker species decreases, we can expect an increased rate of adsorption and thus a larger overshoot. Conversely, increases in the binding energy of the stronger species serve to slow down its adsorption, which again allows the weaker species to attain a greater coverage before being overcome. Similar behaviour is expected and found for the temperature; as the temperature increases, the quantity $\beta\varepsilon$ decreases, predicting a higher rate of adsorption. Thus, the greatest overshoots are achieved in systems with a large ratio of n_A/n_B, a very high binding energy for the stronger species and a very low energy for the weaker one, and a low temperature. The overshoot time depends the most heavily on the temperature of the system, with lower temperatures producing longer overshoot times.

This work has yielded some very interesting results. By selecting adsorbents with the correct binding energies, and using samples at the right temperatures, it should be possible to maximize this overshoot and apply it to kinetic separation, wherein the weaker species would be filtered out. However, before any such application is possible, there is still much more work to be done. In our continuation of this project, we will consider particle-particle interactions between particles in neighbouring sites. We will also investigate the behaviour of systems of pore-like sites to see the effect of diffusion on kinetic selectivity. Finally, we will look at combinations of independent and/or dependent lines of adsorption sites to better represent real systems, which we can then compare to experimental results.

References

Ancilotto, F., Gatica, S., and Cole, M.W. (2005). From one to infinity: Effective dimensionalities of fluids in nanoporous materials. *J. Low. Temp. Phys.*, 138, 201-210.

Burde, J.T. and Calbi, M.M. (2007). Physisorption Kinetics in Carbon Nanotube Bundles. *J. Phys. Chem. C*, 111, 5057-5063.

Calbi, M.M. and Cole M.W. (2002). Dimensional crossover and quantum effects of gases adsorbed on nanotube bundles. *Phys. Rev. B*, 66, 115413.

Calbi, M.M., Cole, M.W, Gatica, S.M., Bojan, M.J. and Stan, G. (2001). Colloquium: Condensed phases of gases inside nanotube bundles. *Rev. Mod. Phys.,* 73, 857-865.

Calbi, M.M. and Riccardo, J.L. (2005). Energy barriers at the ends of carbon nanotube bundles: Effects on interstitial adsorption kinetics. *Phys. Rev. Lett.,* 94, 246103 1-4.

Talapatra, S. and Migone, A.D. (2001). Existence of novel quasi-one-dimensional phases of atoms adsorbed on the exterior surface of close-ended single wall nanotube bundles. *Phys. Rev. Lett.,* 87, 206106 1-4.

Teizer, W., Hallock, R.B., Dujardin, E., Ebbesen, T.W. (1999). ^{4}He desorption from single wall carbon nanotube bundles: A one-dimensional adsorbate. *Phys. Rev. Lett.,* 82, 5305-5308.

Thess, A., et al. (1996). Crystalline Ropes of Metallic Carbon Nanotubes. *Science*, 273, 483-487.

Wilson, T., Vilches, O.E. (2003). Helium adsorbed on carbon nanotube bundles: one-dimensional and/or two-dimensional solids?. *Low Temp. Phys.,* 29, 732-735.